Radiative cascades between Rydberg atomic states

A. B. Kukushkin and V. S. Lisitsa

I. V. Kurchatov Institute of Atomic Energy
(Submitted 1 November 1984)
Zh. Eksp. Teor. Fiz. **88**, 1570–1585 (May 1985)

An analytic expression is derived for two-dimensional radiative cascades between Rydberg atomic states, i.e., for transitions that involve changes in both the principal and the orbital quantum numbers n and l. It is shown that if the familiar Bethe rule is used for the radiative transition probabilities, the population of the levels in the cascade can be described purely classically as a "flow" of the electron fluid in nl-space corresponding to the classical radiative energy and momentum losses. The boundary in nl-space separating the regions of quantum and classical (continuous) electron motion is analyzed, and a general algorithm for calculating the level populations is discussed which is based on the semiclassical method for summing the terms in the cascade matrix. The populations for a photorecombination source are calculated in some specific cases, and the results agree closely with numerical quantum-mechanical calculations even for small n and l. The scaling parameters for the populations are found. The calculations indicate that the populations differ substantially from the statistical-weight distribution, particularly for low temperatures.

1. INTRODUCTION

Many physical applications require the calculation of radiative cascades between highly excited atomic states. Examples include calculations of the populations and line intensities of hydrogen and ionized He II in interstellar gas plasmas (nebulas)[1–3]; spectral line calculations for highly-stripped ions in hot rarefied plasmas whose levels are populated by charge transfer[4] or by dielectronic recombination[5]; level population calculations for atoms excited by stepwise laser transitions,[6] etc.

Techniques for calculating the parameters of radiative cascades were developed by Seaton[1] and are discussed in detail in Ref. 5, Sec. 17. Beigman and Mikhal'chy[7] proposed an analytic computational method which yields results in close agreement with numerical calculations (cf. also Refs. 5 and 8). All of this work deals with one-dimensional radiative cascades, in which the populations f_{nl} of atomic states with different orbital moments l are assumed to be determined by the statistical weights: $f_{nl} = (2l+1)f_n/n^2$. The radiative transitions thus occur between levels with principal quantum numbers n, and the corresponding probabilities $W_{nn'}$ are averaged over the orbital quantum numbers l (this is called the n-method).

Pengelly[2] and Summers[3] have carried out numerical calculations for two-dimensional cascades, i.e., with allowance for the populations of the individual nl-sublevels (this is called the nl-method). Because Summers also considered collisional transitions, it is difficult to follow the chain of cascades using his data.

The amount of data that must be handled and the magnitude of the numerical calculations clearly increase rapidly with n in the nl-method. Approximate methods for treating states with large n thus become essential (cf., e.g., Ref. 2). The error in the approximation increases with n and l, and Pengelly[2] estimates that the error reaches 30% even for relatively small $n = 10$ and $l = 5$. On the other hand, the semiclassical methods should accurately describe the radiative transition probabilities and the bound electronic states for $n \gg 1$ and $l \gg 1$, as is confirmed by the close agreement with quantum-mechanical calculations.[9–11] We therefore expect that models of radiative cascades based on the semiclassical approach will be quite accurate, and the purpose of the present paper is to construct such a model. We will show below that the semiclassical model yields manageable analytic solutions which can be used to identify the parameters in terms of which the numerical data can be interpreted in a consistent, unified way without recourse to laborious numerical methods.

Apart from its "utilitarian" significance, the study of radiative cascades between Rydberg states is of general physical interest for the light it can shed on the relative importance of direct and cascade population and on the dichotomy between the quantum-mechanical and classical descriptions of the electron motion among the levels. Indeed, the problem can be solved in two extreme cases. 1) The nl-state may be assumed to be populated directly by a source q_{nl}, after which it decays with equal probability A_{nl} into all of the lower-lying states; the population will then be equal to $q_{nl} A_{nl}^{-1}$ (this is the direct-population model). 2) One may assume that the electron can reach level nl only by cascading downward through all of the higher-lying states (cascade population model). The latter approach is closely related to the classical concept of motion in nl-space, in which the motion is associated with gradual loss of energy ($E = -1/2n^2$) and momentum [$M = \hbar(l + 1/2)$] at a rate which is determined by classical quantities.[12] Belyaev and Budker[13] employed this classical description in their treatment of radiative cascades; their method is equivalent to using the equation of continuity in phase space for the population $f(E, M)$. On the other hand, the cascade populations were calculated by the n-method in Refs. 7 and 8, where it was shown that the classical "flow" description with respect to the energy variable E is invalid—the electron always moves in quantum-mechanical jumps. It will therefore be of interest to examine the region of nl-space within which the electron can be considered

 0038-5646/85/050937-08$04.00

to move classically; we will investigate this problem in detail.

Photorecombinative population of the atomic states is of particular interest. In this case free electrons with an equilibrium (Maxwellian) distribution fill the states, and the radiative transitions determine both the population source and the subsequent radiative cascades. It is noteworthy that the distribution of the atomic electrons with respect to the orbital number l is by no means always proportional to the statistical weights, even if the source of electrons populating the levels is in equilibrium (cf. the numerical calculations in Ref. 2).

We will examine the classical kinetic equation for radiative cascades in Sec. 2 and consider the quantum-mechanical kinetic equation semiclassically in Sec. 3. The relation of the semiclassical solutions to the cascade matrix formalism used in Refs. 1 and 2 is analyzed in Sec. 4. The level populations for a photorecombination source are calculated analytically in Sec. 5, and the results are used to identify the scaling parameters in Sec. 6, where a detailed comparison with numerical calculations is given. Finally, the results are discussed in Sec. 7.

2. CLASSICAL KINETIC EQUATION

Following Ref. 13, we will use canonically conjugate action-angle variables to analyze the classical kinetic equation for the electron distribution function (DF) in an atom or ion. These variables are convenient because the action variables for a radiating electron vary slowly compared with the orbital period of the electron (the latter is the characteristic time over which the angle variables vary); the DF may therefore be regarded as independent of the angle variables. We take the initial kinetic equation to be the continuity equation in 6-dimensional phase space; after averaging over the angle variables, this equation takes the form

$$\frac{\partial f}{\partial t}+\frac{\partial}{\partial I_k}(\dot{I}_k f)=q, \tag{1}$$

where the I_k are the action variables,

$$I_1=(m\alpha^2/2E)^{1/2}, \quad I_2=M, \quad I_3=M_z, \quad \alpha=Ze^2, \tag{2}$$

and the $\dot{I}_k$ are the corresponding generalized momenta (averaged over the angle variables)[1]:

$$\dot{I}_1=\left|\frac{\partial I_1}{\partial E}\right|\dot{E}, \quad \dot{I}_1=\left(1-\frac{M^2}{3I_1^2}\right)\frac{me^{10}Z^4}{c^3M^5}, \tag{3}$$

$$\dot{I}_2\equiv\dot{M}=-\frac{2}{3}\frac{me^{10}Z^4}{c^3M^2I_1^3}, \quad \dot{I}_3\equiv\dot{M}_z=\frac{M_z}{M}\dot{M}. \tag{4}$$

They give the rates at which a classical radiating electron loses energy and momentum ($\dot{I}_3$ is the rate of change of the z-projection of the momentum).[12]

We will consider only the stationary case in what follows. The spherical symmetry of the Coulomb field implies that the DF f must be independent of M_z.[2)] Equation (1) thus simplifies to

$$\dot{E}\frac{\partial f^{(3)}}{\partial E}+\dot{M}\frac{\partial f^{(3)}}{\partial M}=q^{(3)}. \tag{5}$$

Here the superscript indicates the dimensionality of the space in which f is defined. We note that the phase space variables E, M, and M_z satisfy the classical kinematic constraints

$$M\leqslant M_{max}(E)\equiv(m\alpha^2/2E)^{1/2}, \quad |M_z|\leqslant M.$$

In deriving (5) we have used the important property

$$\mathrm{div}_{(3)}\dot{\mathbf{I}}=0, \tag{6}$$

of the generalized momentum, which implies that the electron flux may be uniform in the space E, M, M_z [$f^{(3)}=$ const satisfies Eq. (1) if $q=0$].

Solving (5) by the method of characteristics, we find

$$f^{(3)}(E,M)=\varphi[M(\tau,E_0)]+\int_{E_0}^{E}q^{(3)}[E',M(\tau,E')]\frac{dE'}{\dot{E}[E',M(\tau,E')]}, \tag{7}$$

where $\varphi(M)$ is the boundary condition for Eq. (5) (we take the boundary to be the line $E=E_0$; the generalization to arbitrary boundaries is evident),

$$\tau\equiv\tau(E,M)\equiv M^{-3}(1-2EM^2/m\alpha^2)\equiv M^{-3}\varepsilon^2, \tag{8}$$

ε is the eccentricity of the electron orbit, and the dependence $M(\tau,E)$ in (7) is determined parametrically by (8). Using (7), we can rewrite the Green function for Eq. (5) in the form

$$G(E'M'\to EM)=\frac{\eta(E-E')}{\dot{E}(E',M')}\delta[M'-M(\tau,E')]\equiv\frac{\eta(M'-M)}{|\dot{M}(E',M')|}\delta[E'-E(\tau,M')], \tag{9}$$

where $\eta=0$ for $x<0$ and $\eta=1$ for $x>0$. The δ-function in (9) corresponds to classical motion of the radiating electrons in the two-dimensional (E,M) space; the trajectories coincide with the characteristic curves of Eq. (5) defined by $\tau(E,M)=$ const. Since the energy loss rate $\dot{I}_1$ exceeds the momentum loss $\dot{I}_2$, ε decreases during the radiation process and the orbits become "rounder."

3. QUANTUM MECHANICAL KINETIC EQUATION IN THE SEMICLASSICAL APPROXIMATION

We will consider the quantum-mechanical kinetic equation for the distribution function $f^{(2)}$ in the two-dimensional space (I_1,I_2) and use the formulas

$$I_1=\hbar n, \quad I_2=\hbar(l+1/2), \quad I_3=\hbar m_z, \tag{10}$$

which relate the action variables to the quantum numbers n, l, and m_z. Because $f^{(3)}$ is independent of M_z, $f^{(2)}$ and $f^{(3)}$ obey the simple relation

$$f^{(2)}(I_1,I_2)=2Mf^{(3)}(I_1,I_2)\equiv(2l+1)f^{(3)}(I_1,I_2). \tag{11}$$

The kinetic equation has the standard form

$$\sum_{n'=n+1}^{\infty}\sum_{l'=l\pm1}f^{(2)}(\Gamma')W(\Gamma'\to\Gamma)+q(\Gamma)=A(\Gamma)f^{(2)}(\Gamma), \quad \Gamma\equiv(n,l), \tag{12}$$

where we have allowed for cascades from higher-lying states; W is the probability per unit time for a radiative transition $\Gamma'\to\Gamma$, q is the external population source, and A is the total rate of radiative decay for the Γ level:

$$A(\Gamma)=\sum_{n'=l+1}^{n-1}\sum_{l'=l\pm1}W(\Gamma\to\Gamma'). \tag{13}$$

For $n \gg 1$ we can replace the sum in (12) by an integration, and $f(\Gamma')$ can be expanded in l near the state Γ for $l \gg 1$. This leads to the integro-differential equation[3)]

$$q + \int_{n+1}^{\infty} \Big[f(n', l) W(n' \to nl) + \frac{\partial f(n', l)}{\partial l} \sum_{\Delta l = \pm 1} (l' - l) W(\Gamma' \to \Gamma) \Big] dn' = A(\Gamma) f(\Gamma), \tag{14}$$

where

$$W(n' \to nl) = \sum_{\Delta l = \pm 1} W(\Gamma' \to \Gamma). \tag{15}$$

The semiclassical kinetic equation (14) reduces to simpler one-dimensional integral or two-dimensional differential equations, depending on the region in the nl-plane, and the solutions can be pieced together uniquely because the corresponding regions overlap.

Indeed, consider (14) for the region $l \ll n$, for which the Kramers approximation is valid for the radiative transition probabilities W. The radiative momentum loss ($\Delta l = \pm 1$) for $l \ll n$ is slower than the energy loss, because transitions with $\Delta n \gg 1$ (including those with $\Delta n \sim n$) are more likely to occur. If the DF f is smooth enough we can therefore discard the differential term in (14), so that l appears merely as a parameter in the resulting integral equation

$$\int_0^{x_m} G_0(x) f\Big[E\Big(1 - \frac{x}{x_m}\Big), M \Big] dx - f(E, M) \int_0^{\infty} G_0(x)\, dx = Q \equiv \frac{\pi q(\Gamma)}{\sqrt{3} A(\Gamma)}, \quad x_m \equiv \frac{(l+1/2)^3}{6n^2}, \tag{16}$$

Here $E = 1/2n^2$ (in atomic units), $M = \hbar(l + 1/2)$, and as before $f(E, M)$ is normalized in Γ space. The function G_0 is related to the leading term in the expansion of the transition probability $W(n' \to nl)$ [Eq. (15)] with respect to $\hbar$ for $l \ll n$ (cf. Refs. 10 and 11):

$$G_0(x) = x[K_{1/3}^2(x) + K_{2/3}^2(x)]. \tag{17}$$

The function $A(\Gamma)$ corresponding to (17) is the total radiative decay rate for the level $\Gamma = \{n, l\}$,

$$A(\Gamma)_{\text{a.u.}} = 4[\sqrt{3}\pi c^3 n^3 (l+1/2)^2]^{-1}. \tag{18}$$

The first (cascade) integral in (16) is negligible for small x_m, so that the population of level Γ is determined by the contribution from direct population by the external source q, $f(\Gamma) = q(\Gamma)/A(\Gamma)$. The cascade term becomes important as x_m increases.

The kernel of the integral equation (16) depends on x only through the difference $1 - x/x_m$, because the Kramers transition probability W depends only on the energy difference between the initial and final states; we can therefore solve Eq. (16) by taking Laplace transforms. The latter satisfy the equation

$$\bar{f}(s) = \bar{Q}(s)/s\bar{G}_2(s), \tag{19}$$

where s is the Laplace variable conjugate to x_m,

$$G_2(x) = \int_x^{\infty} G_0(x')\, dx' = xK_{1/3}(x) K_{2/3}(x), \qquad s\bar{G}_2(s) = \bar{G}_0(0) - \bar{G}_0(s). \tag{20}$$

We can approximate G_2 to within 10% by the expression

$$G_2(x) \approx \alpha \exp(-2x), \quad \bar{G}_2(s) = \alpha(s)/(s+2), \tag{21}$$

where the function $\alpha(s)$ is slowing varying, $\alpha(s = 0) = \pi^2/6 = 1.64$; $\alpha(s = \infty) = \pi/\sqrt{3} = 1.81$. If we set $\alpha = 1.7$, ensuring at most a 10% error in (21), we get the approximate analytic expression

$$f(\Gamma) = \frac{q(\Gamma)}{A(\Gamma)} + \int_{n+1}^{\infty} \frac{q(n', l)}{|\dot{n}(n', l)|} dn', \tag{22}$$

for an arbitrary source q; here the quantity $\hbar\dot{n} \equiv \dot{I}_1$ gives the rate of energy loss $\dot{E}$ [Eq. (3)] for $l \ll n$.

Equation (21) embodies the semiclassical approximation for G_2. Indeed, (21) together with (20) implies that $G_0(x) = 2G_2(x)$; for comparison, the exact result is

$$G_0(x) - 2G_2(x) = x(K_{1/3}(x) - K_{2/3}(x))^2 \equiv D(x) \equiv \text{BC}. \tag{23}$$

The correction $D(x)$ is proportional to the (Kramers) transition probability for a transition with $\Delta l = -\operatorname{sgn}(\Delta n)$, i.e., for transitions when the change in l is opposite to the change in the principal quantum number n. Bethe established empirically[14] that such transitions are actually somewhat less likely than transitions with $\Delta l = \operatorname{sgn}(\Delta n)$, and the magnitude of the suppression increases with Δn (this effect is discussed heuristically in Ref. 10 for $n \gg 1$, $l \gg 1$). These transitions are essentially quantum-mechanical in nature, since both n and l decrease in the classical treatment. The semiclassical approximation thus consists in neglecting $D(x)$ in (23), which we may call the Bethe correction (BC). Numerical calculations of the ratio D/G_2 reveal that the Bethe correction becomes significant only for very small $x \lesssim 10^{-2}$ and thus provide a numerical justification for the Bethe rule. The semiclassical approximation is therefore quite generally valid for $x \gtrsim 10^{-2}$.

The DF (22) satisfies Eq. (14) for $x_m \lesssim 1$ (including $x_m \ll 1$), where the two integrals in (16) have the same order of magnitude. The integrals cancel for $x_m \gg 1$, which corresponds to the classical limit in Eq. (12). We can follow this transition by expanding $f(\Gamma')$ in the integrand with respect to both n and l [cf. (14)]. This expansion, which is valid for $x_m \gg 1$, leads to the two-dimensional differential equation

$$\dot{E} \frac{\partial f^{(2)}}{\partial E} + \dot{M} \frac{\partial f^{(2)}}{\partial M} - \frac{\dot{M}}{M} f^{(2)} = q^{(2)} \tag{24}$$

for $f^{(2)}(\Gamma)$; recalling (11), we see that (24) is equivalent to Eq. (5).

We note that since the classical limit is consistent with the inequality $l \ll n$, it should be describable in terms of the Kramers transition probabilties W. The leading terms in the

$\hbar$-expansion for the transition probability vanish because of the above-mentioned cancellation between the cascade and direct-population terms; it is thus necessary to examine the first-order quantum-mechanical correction to the classical probability W which was calculated in Ref. 11. This correction corresponds to the third term in the left-hand side of Eq. (24), so that failure to include this correction will cause a superfluous term to be present in (5). We give an explicit expression for W in Appendix I.

As $\hbar \to 0$, a continuous classical flow of electrons described by Eq. (24) thus replaces the discrete quantum-mechanical motion specified by the nonlocal coupling in the integral equation (16).

We will now consider how the semiclassical and classical distributions (22) and (7) are to be matched. Comparison in the Kramers region $l \ll n$ shows that the first term in (7) (the contribution from the boundary condition) must be replaced by the contribution from direct population. The resulting distribution function is valid for the entire semiclassical range of n and l, including the non-Kramers region $l \sim n$:

$$f(\Gamma)=\frac{q(\Gamma)}{A(\Gamma)}+M\int_{n+1}^{\infty}\frac{q[n',l(\tau,n')]dn'}{|\dot{n}[n',l(\tau,n')]|M(\tau,n')}$$

$$\equiv\frac{q}{A}+\hat{C}[q], \tag{25}$$

where $l(\tau,n)$ is given by (8). Indeed, the boundary condition contributes to the classical distribution (7) mostly for large n and small x_m, for which a purely classical description breaks down. In Sec. 6 we will carry out calculations for a specific (photorecombination) source and piece the solutions together explicitly; the results will confirm the correctness of the semiclassical expression (25).

4. RELATIONSHIP OF THE SEMICLASSICAL SOLUTION TO THE QUANTUM-MECHANICAL CASCADE MATRIX. ALGORITHM FOR FINDING THE GENERAL SOLUTION

We will interpret the above result by using the quantum cascade matrix formalism, in which the cascade matrix $C(\Gamma'\to\Gamma)$ plays the role of the Green's function for the quantum-mechanical equation (12). The DF solving (12) can be expressed in the form[1,2,5]

$$f(\Gamma)=A^{-1}(\Gamma)\sum_{n'=n}^{\infty}\sum_{l'=0}^{n-1}C(\Gamma'\to\Gamma)q(\Gamma')\equiv\frac{q(\Gamma)}{A(\Gamma)}$$
$$+\frac{1}{A(\Gamma)}\sum_{n'=n+1}^{\infty}\sum_{l'=0}^{n-1}C(\Gamma'\to\Gamma)q(\Gamma'). \tag{26}$$

The C-matrix can be regarded as the probability of a $\Gamma'\to\Gamma$ transition via all possible cascades [$C(\Gamma\to\Gamma)=1$] and obeys the two equivalent recursion formulas

$$C(\Gamma'\to\Gamma)=\sum_{n''=n}^{n'-1}\sum_{l''=l'\pm1}\frac{W(\Gamma'\to\Gamma'')}{A(\Gamma')}C(\Gamma''\to\Gamma)$$
$$\equiv\sum_{n''=n+1}^{n'}\sum_{l''=l\pm1}C(\Gamma'\to\Gamma'')\frac{W(\Gamma''\to\Gamma)}{A(\Gamma'')}. \tag{27}$$

Comparison of (26) with the semiclassical function (25) shows that the cascade population will be purely classical if f in (12) is smooth enough [so that $f(\Gamma')$ can be expanded as a Taylor series for $\Gamma'\approx\Gamma$]. In the classical limit, C takes the form

$$C(\Gamma'\to\Gamma)\propto MA(\Gamma)\delta(\tau-\tau'),$$

where τ [cf. (8)] describes the classical trajectory. A similar expression for C also follows directly from Eqs. (27) in the classical limit—if we let $\hbar\to0$ as in the derivation of Eq. (24), we find that $C(\Gamma'-\Gamma)\propto MA(\Gamma)\mathcal{F}(\tau,\tau')$, where the function $\mathcal{F}$ is arbitrary.

We will now estimate the error in the classical description of cascades for arbitrary sources q [including selective population sources $q\propto\delta(\Gamma-\Gamma_0)$] by substituting the approximate solution (22) for $n\ll l$ into the corresponding equation. The noncanceling term can be transformed into

$$\int_0^{x_m}\frac{q(E',M)}{A(E',M)}\left[G_0(x)-\frac{4\sqrt{3}}{\pi}G_2(x)\right]dx,$$

$$x=\left[\frac{(E-E')M^3}{3}\right]_{\text{a.u.}}. \tag{28}$$

The expression in square brackets in the integrand coincides with the Bethe correction (23) to within 10%. Equation (28) implies that the terms in the square brackets cancel only for those x for which the Bethe correction can be neglected. The distribution function $f(\Gamma)$ given by (25) cannot be used for sources q whose main contribution to the integral in (28) comes from small x, for which the terms in square brackets do not cancel.

In what follows we will assume a δ-function source. Equation (25) is clearly inapplicable if direct transitions from the level Γ populated by the source are important (this corresponds to the leading term in the Bethe correction as $x\to0$). In any case, such direct transitions will be important for levels Γ' close to Γ, as well as for more remote levels that are populated solely by BC-transitions, i.e., by electrons lying far from the classical trajectory. Classical cascades may occur between levels which lie close to the classical trajectory provided they are sufficiently far from the levels Γ populated by the source ($\Delta x_m\gtrsim1$). The quantum→classical transition in this case can be described in terms of a modified classical cascade. For example, in the Kramers region this gives

$$f=\frac{q}{A}+\int_{n+1}^{\infty}\frac{q(n',l)}{|\dot{n}(n',l)|}\frac{G_0(x)}{2G_2(x)}dn',\quad x=\left[\frac{(E-E')M^3}{3}\right]_{\text{a.u.}}. \tag{29}$$

However, there is an alternative, more systematic method for treating the "quantum mechanical" properties of the source. This method exploits the fact that the form of the quantum-mechanical kinetic equation remains unchanged if we subtract arbitrarily many of the leading terms in the expansion of the distribution function in powers of $\Gamma'-\Gamma$ (here $\Gamma'=(n',l')$ is an arbitrary level populated by the source and $\Gamma=(n,l)$ is the final level in the cascade). Indeed, Eq. (12) continues to hold for $f-q/A$ if we replace q by

$$\langle q\rangle \equiv \sum_{n'=n+1}^{\infty} \sum_{\Delta l=\pm 1} q(\Gamma') \frac{W(\Gamma' \to \Gamma)}{A(\Gamma')} . \tag{30}$$

Proceeding as in Sec. 3, we thus arrive at the distribution function

$$f = \langle f\rangle \equiv q/A + \langle q\rangle/A + \hat{C}[\langle q\rangle], \tag{31}$$

which may be compared with (25). The general result is

$$f = \langle f\rangle_N \equiv \frac{q}{A} + A^{-1} \sum_{i=1}^{N} \langle q\rangle_i + \hat{C}[\langle q\rangle_N], \tag{32}$$

where the effective source $\langle q\rangle_N$ describes the population of the level Γ by all N-stage (N-photon) cascade transitions from all points of the source,

$$\langle q\rangle_N = \sum_{n_1=n+N}^{\infty} \sum_{n_2=n+N-1}^{\infty} \cdots \sum_{n_N=n+1}^{\infty} \sum_{l_1,\ldots,l_N=0}^{n_l-1}$$

$$\times q(\Gamma_1) \frac{W(\Gamma_1 \to \Gamma_2)}{A(\Gamma_1)} \cdots \frac{W(\Gamma_N \to \Gamma)}{A(\Gamma_N)} \tag{33}$$

and the appropriate selection rules must be used in calculating the radiative transition probabilities $W(\Gamma_i \to \Gamma_{i+1})$. Each additional summation in (33) smooths the effective source further and thus decreases the error caused by summing the remainder terms in the series "classically" to $\approx 10\%$ (cf. Sec. 3). The error in the final result depends both on the specific form of q and on n, l. The error will be small if the neglect of an additional term corresponding to an $(N+1)$-stage cascade $\Gamma' \to \Gamma$ produces little relative change in $f(\Gamma)$. The above algorithm can be used to calculate f for radiative electron cascades between Rydberg atomic or ionic states for arbitrary sources and quantum numbers (in particular, n and l may be small).

We note that the extent to which the population source is "quantum mechanical" depends partly on how "spread out" it is [cf. (27)] and partly on the range of values n, l in which the source is concentrated. For example, the DF is highly quantum mechanical if a distributed "classical" source is concentrated in the "quantum" region $x_m \ll 1$ (cf. Sec. 5). On the other hand, the cascade population can be described classically even for a selective source if the latter is concentrated in the "classical" region $l \sim n$. Thus, if the levels with $l = n-1$ are selectively populated by the source, the population of the lower levels by cascades can be described purely classically and the result agrees with the exact quantum-mechanical expression. Specifically, if we use the quantum cascade matrix and recall the relations

$$|\dot{n}| = |\dot{l}| = A(n, l) = W(n, l \to n-1, l-1) = {}^2/_3 n^{-5},$$

we find from (26) that

$$f(n, l) = q(n_0, l_0) A^{-1}(n, l) \delta_{n, n_0-k} \delta_{l, l_0-k},$$

where δ is the Kronecker symbol and $k \geqslant 0$. A calculation using Eq. (25) leads to the same result.

5. POPULATIONS FOR A PHOTORECOMBINATION SOURCE

We will now use the results in Secs. 3 and 4 to calculate the level populations for a Rydberg atom populated by a photorecombination source. Since the same radiative transitions are involved in both cases, the above approximations for cascades can also be applied to the photorecombination source. This will enable us to relate the error in the approximation (21) to the error in the semiclassical DF (25) in a specific case.

We begin by calculating the populations in the Kramers region $l \ll n$. If the atomic levels are populated by phototransitions of free electrons with a Maxwellian DF

$$f_M^{(2)} = 2M\bar{A} \exp(-\mathscr{E}/T), \quad \bar{A} = (2\pi m T)^{-3/2}$$

we have [cf. (16)]

$$Q(\Gamma) = \int_{x_m}^{\infty} f_M^{(2)}\left(E\left(\frac{x}{x_m} - 1\right), M\right) G_0(x)\, dx = 2M\bar{A}\left\{ G_2(x_m) \right. \tag{34}$$

$$\left. - \exp(E/T) x_T \int_{x_m}^{\infty} G_2(y) \exp(-y x_T)\, dy \right\}, \quad x_T \equiv \left[\frac{3}{TM^3}\right]_{\text{a.u.}} .$$

Using (21) to evaluate (34), we get $Q \approx 2(2+x_T)^{-1} G_2(x_m)$. However, this result is invalid for small x_m and large x_T, i.e., in the "quantum" region in which the Bethe correction $D(x)$ cannot be neglected. Indeed, the singularity in G_0 is important here and substantially determines the value of the entire integral with respect to x. If we separate out the contribution from this singularity, (34) becomes

$$Q(\Gamma) = \frac{2}{2+x_T} G_2(x_m) + \frac{x_T}{2+x_T} \psi \exp(E/T), \tag{35}$$

$$\psi = \int_{x_m}^{\infty} D(y) \exp(-y x_T)\, dy, \tag{36}$$

where we can now approximate G_2 by (21). Equations (35) and (36) show that as expected (cf. Sec. 3), using (21) is equivalent to neglecting the Bethe correction (23) in the source.

We will next calculate the DF (22) for a source (35); this corresponds to including the Bethe correction in the source but neglecting it in the Green function for Eq. (16). It will be helpful to express the result in the form

$$f(\Gamma) \equiv 2\bar{A}M \exp(E/T)\, b(\Gamma),$$

so that $f(\Gamma)/b(\Gamma)$ coincides with the equilibrium distribution ($E > 0$). Here b is given by

$$b(\Gamma) \equiv b_{nl} = \frac{2}{2+x_T} \exp(-E/T) + \frac{1}{\alpha} \psi(x_m, x_T), \tag{37}$$

and ψ and α are defined by (36) and (21). The function D can be simplified in various ways, depending on the values of n,l; ψ can then be expressed in terms of exponential integrals and incomplete gamma-functions (Appendix II).

For $n, l \gg 1$, the second term in b_{nl} [Eq. (37)] is important only for $x_m \ll 1$, $x_T \gg 1$; f is therefore independent of the energy E at the edge of the Kramers region, where $l \sim n (x_m \gtrsim 1)$. This implies that the solution outside the Kramers region can be found from the first term in (37), regarded simply as a classical boundary condition. Because this term is independent of E, the resulting DF will be the same regardless of which line in nl-space is chosen as the

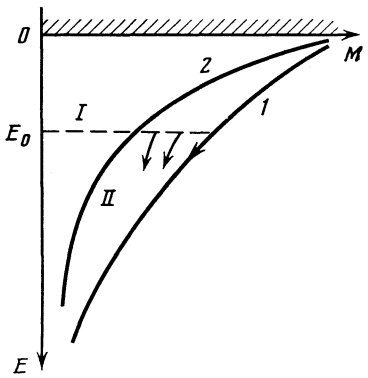

FIG. 1. Regions in the E, M plane corresponding to semiclassical (I) and classical electron motion (II). Curve 1 demarcates the region of classically allowed motion: $2EM^2 = 1$ [$M = M_{\max}(E)$]; curve 2 separates regions I and II: $EM^3 \sim 1$ ($x_m \sim 1$). The arrows indicate the classical trajectories [the characteristics of Eq. (5)]; the classical boundary conditions are imposed on the line $E_0 = \text{const}$.

boundary. If we then use (7), (8) to continue (37) along the characteristic curve, we get the final result

$$b_{nl} = \frac{2}{2+x_T\varepsilon^2}\exp(-E/T) + \frac{1}{\alpha}\psi(x_m, x_T), \tag{38}$$

which is valid for all semiclassical n,l. We are able to continue the solution in this way because the source (35) is concentrated in the Kramers region, so that there is no need to evaluate (25) directly (recall that A and $\dot{n}$ there involve the transition probabilities for arbitrary l/n). Indeed, a calculation using (25) for $(l/n - 1) \ll 1$ reveals that these states are populated solely by classical cascades; moreover, most of the contribution comes from transitions far from the curve $l \sim n$. The latter result corresponds precisely to the classical behavior, in which the states near the boundary $M = M_{\max}(E)$ (Fig. 1) can be populated by a source concentrated in a region with eccentricity $\varepsilon \to 1$ (Sec. 2). For a photorecombination source, the Kramers region shrinks along the n axis as l increases (as the edge of the continuum is approached) and thus is effectively transformed into a boundary condition.

We will now show that the algorithm in Sec. 4 in fact incorporates some additional Bethe corrections to the DF. For a singly averaged source ($N = 1$), (30) gives

$$\langle Q\rangle \equiv \langle q\rangle/A = \frac{3}{\pi^2}\int_0^{x_m} G_0(x)\,Q(x_m - x)\,dx; \tag{39}$$

to within the 10% error in approximating the coefficient α in (21), this gives

$$\langle f\rangle = f + \frac{3}{\pi^2}\int_0^{x_m} D(x)\,Q(x_m - x)\,dx, \tag{40}$$

for $\langle f\rangle$ in (31); here f is defined by (25). A calculation of $\langle f\rangle$ for our photorecombination source reveals that the Bethe corretions are smaller than the 10% error in (21). Thus, if we include the linear corrections to (37) in (40), we find that

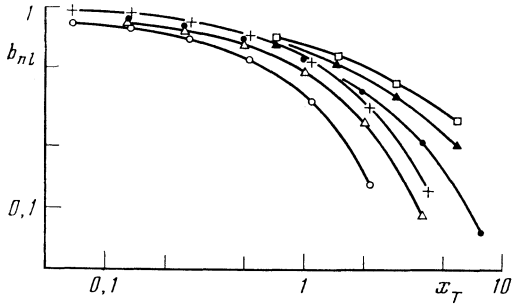

FIG. 2. Atomic level populations from Ref. 2 replotted as a function of the parameter $x_T = 3/TM^3$ for several values of $x_m = EM^3/3$: ○, $x_m = 0.77$; △, 0.42; +, 0.28; ●, 0.15; ▲, 0.072; □, 0.026.

$$\langle b\rangle = \frac{2}{2+x_T}\left[1 + \exp(-2x_m) - \frac{\sqrt{3}}{\pi}G_2(x_m)\right]\exp\left(-\frac{E}{T}\right) + \frac{\psi}{\alpha}\left[1 + \frac{x_T}{(2+x_T)\alpha}\int_0^{x_m} D(x)\,dx\right]. \tag{41}$$

Since the factor multiplying ψ is significant only for $x_m \ll 1$, $x_T \gg 1$, we conclude as in Sec. 4 that the error Eq. (37) for b (Γ) is 10%, the same as in (21).

6. SCALING LAWS. COMPARISON WITH NUMERICAL QUANTUM-MECHANICAL CALCULATIONS

The semiclassical DF (38) derived above can be used to establish approximate scaling laws for the level populations. These laws are a consequence of the fact that $f(\Gamma)$ in (38) depends on fewer variables than is the case for the quantum-mechanical DF. Indeed, f_{nl} depends only on x_m and x_T for $x_m \ll 1$, $x_T \gg 1$. If one of the parameters x_m or x_T^{-1} becomes ~ 1, the second term in (38) is much less than the first and f depends only on x_T. Elsewhere in nl-space, f depends on the parameter $x_T\varepsilon^2$. We thus have a smooth transition between three scaling laws for $n,l \gg 1$. Comparison of the semiclassical DF (38) with the results of numerical quantum-mechanical calculations[2] reveals that the semiclassical DF can also be used for relatively small n and l (cf. the remark in Sec. 1).

We will use the numerical data in Ref. 2 to check the similarity rules implied by the semiclassical method; according to Fig. 2, these data depend smoothly on x_T for $x_m = \text{const}$. Figure 3 gives a particularly striking illustra-

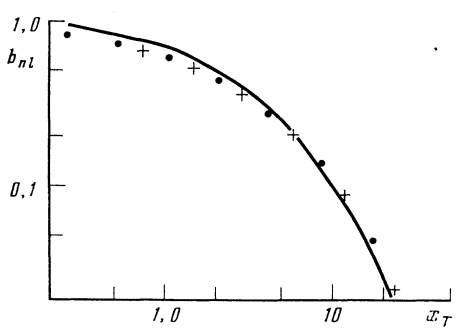

FIG. 3. Universal dependence of the level populations b_{nl} from (38) as a function of the parameter $x_T = 3/TM^3$ (solid curve); the points ● and + show the numerical values calculated in Ref. 2 for the states $n = 10$, $l = 3$ and $n = 6$, $l = 2$, respectively ($x_m = 0.072$).

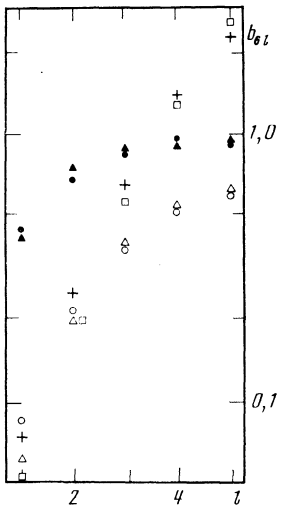

FIG. 4. The populations b_{6l} for an $n = 6$ hydrogen level as a function of the orbital quantum number l for several temperatures. $T = 8 \cdot 10^4$ K: ●, numerical data from Ref. 2; ▲, calculated from Eq. (38). $T = 10^4$ K: ○, Ref. 2; △, Eq. (38). The points + and □ give $10^2\, b$ from Ref. 2 and Eq. (38), respectively, for $T = 1/8 \cdot 10^4$ K.

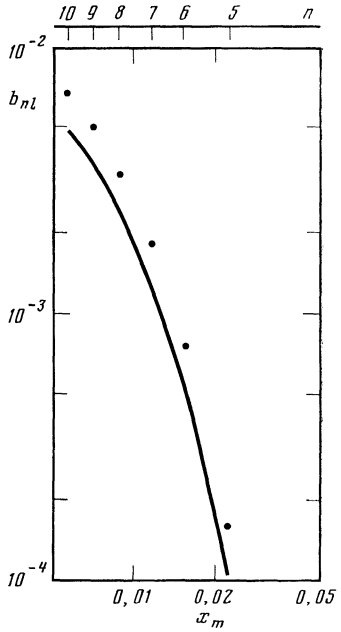

FIG. 5. The level populations b_{nl} as a function of the parameter $x_m = EM^3/3$ for fixed $x_T = 214$ ($T = 1/8 \cdot 10^4$ K, $l = 1$); x_m was varied by changing the principal quantum number n (top scale). The points ● show numerical values from Ref. 2; the curve was calculated using Eq. (38).

tion of the accuracy of the semiclassical result. The symbols ● and + in Fig. 3 indicate values taken from Ref. 2 as functions of x_T for the two states $n = 6$, $l = 2$ and $n = 10$, $l = 3$, for which x_m ($= 0.072$) and ε^2 (≈ 0.83 and 0.87) are similar. We see that although these values correspond to different n,l, they lie on a single curve which coincides to within 20% with the semiclassical result (38).

The population distribution with respect to the orbital quantum number l is also of interest. Figure 4 plots the relative populations b as functions of l for several different temperatures. We see that, as noted in Sec. 1, the dependence $b(l)$ in general differs from the statistical-weight distribution corresponding to $b(l) = \text{const}$—for low temperatures (large x_T) $b(l)$ increases much more sharply with l, while for large T (small x_T) $b(l) \approx \text{const}$. These results clearly agree with the semiclassical formula (38).

Finally, the similarity law with respect to x_m is illustrated in Fig. 5, which plots b_{nl} for $l = 1$ (the p-state) as a function of x_m for $n = \text{const}$. We see that even for these small values of l, the semiclassical formula (38) agrees to within 35% with the quantum mechanical calculations in Ref. 2.

We can also use Eq. (22) to illustrate the relative importance of direct and cascade population in the Kramers region for a photorecombination source; we find

$$f_c \propto \frac{2}{2+x_T}(1-\exp(-2x_m)) + \frac{2}{2+x_T}\frac{\psi}{\alpha}\exp(E/T),$$
$$f_D \propto \frac{2}{2+x_T}\exp(-2x_m) + \frac{x_T}{2+x_T}\frac{\psi}{\alpha}\exp(E/T) \qquad (42)$$

for the cascade and direct populations f_c and f_D. The contribution from f_D clearly decreases as x_m increases, and the sum $f_c + f_D$ coincides with (37). The numerical values of $f_D/(f_D + f_c)$ agree reasonably well with the data in Ref. 2—for $n = 6$ and $T = 10^4$ K, e.g., (42) implies that $f_D(f_D + f_c)$ is equal to 96% for $l = 1$ and 87% for $l = 2$; the corresponding values from Ref. 2 are 81% and 73%.

The momentum-averaged dependences $f(n)$ are also of interest. The major contribution to the integral over l comes from the first term in (38), which gives

$$\frac{f(n)}{n^2} \propto \int_0^1 x\left[1+\frac{3(1-x^2)}{2Tn^3x^3}\right]^{-1} dx \approx \begin{cases} 1/2, & Tn^3 \gg 1 \\ \dfrac{Tn^3}{3}\ln\dfrac{3}{Tn^3}, & Tn^3 \ll 1 \end{cases} \qquad (43)$$

We see that $f(n)$ depends on the product Tn^3 (this result differs from the dependence on Tn^2 found by the n-method[1,8]).

CONCLUSIONS

The above semiclassical method for calculating the atomic level populations for multistage radiative cascades yields results accurate to within 10%. The most difficult step in the numerical calculations is to sum the contributions from the various transitions. Indeed, the δ-function properties of the cascade matrix that correspond to radiating electrons moving along characteristics in the classical region [cf. (27)] are difficult to discern numerically. For example, the calculations in Ref. 2 detected only the boundary characteristic corresponding to $l = l_{\max} = n - 1$.

The algorithm in Sec. 4 for calculating the population in the quantum case for arbitrary sources can thus be used to treat cascades through arbitrarily many Rydberg states. The number of quantum-mechanical cascade transitions which cannot be described classically may be quite small in prac-

tice, particularly for distributed sources. For example, the cascade population is purely classical for a photorecombination source (Secs. 5,6).

Expression (38) for the DF for a photorecombination source is directly related to the "effective" recombination coefficient[2] that accounts for both direct and cascade population of levels. Equations (35) and (36) describe direct population by phototransitions from a Maxwellian continuum. Appendix II gives an analytic approximation for the function ψ associated with the "Bethe correction" (Sec. 3); this approximation makes it relatively easy to calculate the rate of direct photorecombination.

We thank I. L. Beĭgman and I. I. Sobel'man for valuable discussions.

APPENDIX I

Equations (28)–(30) in Ref. 11 lead to the explicit form

$$W_{\text{a.u.}}(nl\to n'l') = \delta_{\Delta l,\pm 1}\frac{2(l+^1/_2)}{3\pi^2 c^3 (nn')^3}x\left\{(K_{^1/_3}(x)-\Delta l K_{^1/_3}(x))^2+\frac{\hbar}{5M}\tilde{\Phi}(x,\Delta l)\right\} \tag{I.1}$$

for the probability W of a Kramers ($l\ll n$, $\omega n^3\gg 1$) radiative transition in a Coulomb field, including the first quantum correction to the classical limit. Here δ is Kronecker's symbol, $\Delta l = l' - l$, $x = (\omega M^3/3)_{\text{a.u.}} \equiv [(E_\eta - E_{\eta'})(l+1/2)^3/3]_{\text{a.u.}}$, and the quantum correction $\tilde{\Phi}$ is of the form

$$\tilde{\Phi}(x,\Delta l) = K_{^1/_3}^2(x)[33x+(7+18x^2)\Delta l] + K_{^2/_3}^2(x)[27x+18x^2\Delta l] - K_{^1/_3}(x)K_{^2/_3}(x)[7+36x^2+60x\Delta l]. \tag{I.2}$$

An expression is also required for the probability $W(n'l'\to nl)$ for the backward transition as a function of x; it can be derived as in (I.1), (I.2) by recalling the relation between the arguments x and $x' = [(E_\eta - E_{\eta'})(l'+1/2)^3/3]_{\text{a.u.}}$.

APPENDIX II

The function $D(x)$ in (23) (the "Bethe correction") must first be approximated before we can find an approximate analytic formula for ψ in (36); we recall that ψ appears in Eq. (35) for the rate of population of atomic states by photorecombination transitions from a Maxwellian continuum. It is helpful here to express the modified Bessel functions in terms of the Airy function (cf., e.g., Ref. 15):

$$D(x) \equiv x(K_{^1/_3}(x)-K_{^2/_3}(x))^2 = \frac{2\pi^2}{x^{^1/_3}}\left(\frac{2}{3}\right)^{^1/_3}[\sqrt{z}\,\mathrm{Ai}(z)-\mathrm{Ai}'(z)]^2, \quad z=\left(\frac{3x}{2}\right)^{^2/_3}, \tag{II.1}$$

where derivatives are indicated by a prime. Using the tabulated values for Ai and Ai' in Ref. 15, we then get the approximations

$$\begin{aligned} D(x) &= 1{,}15\frac{1-2{,}7x^{^1/_3}}{x^{^1/_3}}, && 0\leqslant x\leqslant 5\cdot 10^{-3}\equiv C_1,\\ D(x) &= 0{,}11x^{-^2/_3}, && C_1\leqslant x\leqslant 3\cdot 10^{-2}\equiv C_2,\\ D(x) &= 3{,}45\cdot 10^{-2}x^{-1}, && C_2\leqslant x\leqslant 0{,}1\equiv C_3,\\ D(x) &= 4{,}8\cdot 10^{-2}x^{-1}\exp(-2{,}8x), && C_3\leqslant x, \end{aligned} \tag{II.2}$$

which are accurate to 5% for the x values of importance in the integral in (36). The desired approximation

$$\psi = \eta(C_1-x_m)J_1+\eta(C_2-x_m)J_2(\max\{C_1,x_m\}) + \eta(C_3-x_m)J_3(\max\{C_2,x_m\})+J_4(\max\{C_3,x_m\}), \tag{II.3}$$

then follows from (II.2); $\eta = 0$ for $x<0$ and $\eta = 1$ for $x>0$, and the functions J_k are defined by

$$\begin{aligned} J_1 &= \frac{1{,}15\Gamma(^2/_3)}{x_T^{^2/_3}}\left[I\left(C_1x_T,\frac{2}{3}\right)-I\left(\frac{E}{T},\frac{2}{3}\right)\right] + \frac{3{,}1}{x_T}(e^{-C_1x_T}-e^{-E/T}),\\ J_2(x) &= \frac{0{,}11\Gamma(^1/_3)}{x_T^{^1/_3}}\left[I\left(C_2x_T,\frac{1}{3}\right)-I\left(x_Tx,\frac{1}{3}\right)\right],\\ J_3(x) &= 3{,}45\cdot 10^{-2}[E_1(x_Tx)-E_1(C_3x_T)],\\ J_4(x) &= 4{,}8\cdot 10^{-2}E_1((2{,}8+x_T)x). \end{aligned} \tag{II.4}$$

Here $E_1(x)\equiv -Ei(-x)$ is the exponential integral function and $I(x,m)$ is related to the incomplete gamma-function by

$$I(x,m) = \Gamma^{-1}(m)\int_0^x e^{-t}t^{m-1}\,dt. \tag{II.5}$$

The extensive tabulations of E_1 and $I(x,m)$ in Refs. 16 and 17, respectively, are helpful in calculations.

[1)]Here and below, $E>0$ is the negative of the total energy of the bound electron.
[2)]We assume that q is independent of M_z.
[3)]We will henceforth write f in place of $f^{(2)}$ where no confusion can result.

[1]M. J. Seaton, Mon. Not. R. Astron. Soc. **119**, 90 (1959).
[2]R. M. Pengelly, Mon. Not. R. Astron. Soc. **127**, 145 (1964).
[3]H. P. Summers, Mon. Not. R. Astron. Soc. **178**, 101 (1977).
[4]V. A. Abramov, F. F. Baryshnikov, A. I. Kazanskii, *et al.*, in Voprosy Teorii Plazmy (Reviews by Plasma Physics), B. B. Kadomtsev, ed., Vol. 12, Energoatomizdat, Moscow (1982), p. 94.
[5]L. A. Vaĭnshteĭn, I. I. Sobel'man, and E. A. Yukov, Vozbuzhdenie Atomov i Ushirenie Spektral'nykh Liniĭ (Atomic Excitation and Spectral Line Broadening), Nauka, Moscow (1979).
[6]B. K. Smirnov, Vozbuzhdennye Atomy (Excited Atoms), Energoizdat, Moscow (1982).
[7]I. L. Beigman and E. D. Mikhal'chy, J. Quant. Spectr. Rad. Trans. **91**, 365 (1969).
[8]I. L. Beĭgman and I. M. Gaĭsinskiĭ, FIAN Preprint No. 181 (1979).
[9]V. M. Katkov and V. M. Strakhovenko, Zh. Eksp. Teor. Fiz. **75**, 1269 (1978) [Sov. Phys. JETP **48**, 639 (1978)].
[10]S. P. Goreslavskiĭ, N. B. Delone, and V. P. Kraĭnov, Zh. Eksp. Teor. Fiz. **82**, 1789 (1982) [Sov. Phys. JETP **55**, 1032 (1982)]; FIAN Preprint No. 33 (1982).
[11]V. I. Kogan and A. B. Kukushkin, Zh. Eksp. Teor. Fiz. **87**, 1164 (1984) [Sov. Phys. JETP **60**, 665 (1984)].
[12]L. D. Landau and E. M. Lifshits, Teoriya Polya (The Classical Theory of Fields), 4th ed., Pergamon Press, Oxford (1975).
[13]S. T. Belyaev and G. I. Budker, in: Fizika Plazmy i Problema UTR (Plasmas Physics and the Problem of Controlled Thermonuclear Reactions), Vol. 3, M. A. Leontovich, ed., Izd. AN SSSR, Moscow (1958), p. 46.
[14]H. A. Bethe and E. E. Salpeter, *Quantum Mechanics of One- and Two-Electron Systems*, Springer Verlag, New York (1958).
[15]M. Abramowitz and I. A. Stegun, eds. Handbook of Mathematical Functions, Dover, New York (1965).
[16]V. I. Pagurova, Tablitsy Integro-Éksponential'noĭ Funktsii (Tables of the Exponential Integral Function), Izd. Vychisl. Tsentra AN SSSR, Moscow (1959).
[17]V. I. Pagurova, Tablitsy Nepolnoĭ Gamma-Funktsii (Tables of the Incomplete Gamma-Function), Izd. Vychisl. Tsentra AN SSSR, Moscow (1963).

Translated by A. Mason